

Morphologies and Miscibilities of Polypropene with Random Poly(ethene-co-1-butene).

Yi Thomann, Jürgen Suhm, Ralf Thomann, Ralf-Dieter Maier, Rolf Mülhaupt, Georg Bar*

Freiburger Materialforschungszentrum and Institut für Makromolekulare Chemie, Albert-Ludwigs-Universität, 79104 Freiburg, Germany

SUMMARY: We investigated the miscibilities and morphologies of isotactic and syndiotactic polypropenes (i-PP/s-PP) with random poly(ethene-co-1-butene) (PEB) as a function of 1-butene content in PEB. The blend samples were studied by means of phase imaging atomic force microscopy, transmission electron microscopy, differential scanning calorimetry, dynamic mechanical analysis and X-ray scattering. It was found that i-PP is melt miscible with PEB for 1-butene contents of ≈ 88 wt.-% (miscibility window). Partial miscibility was found for s-PP/PEB blends for 1-butene contents ranging from 50 - 88 wt.-%.

Introduction

For past several years, the morphologies and miscibility behavior of polyolefin blends have been studied experimentally and theoretically.¹⁻⁸⁾ In particular, there has been significant fundamental and industrial interest in blends of polypropene (PP) with elastomeric polyolefins. It is well known that blending of PP with ethene/1-olefin copolymers influences strongly the morphology and mechanical properties of such blends.^{9,10)} In general, the mechanical properties of polymer blends are governed by miscibility or compatibility of the polymer components and therefore by composition, morphology and interface structure. The miscibility and compatibility of PP with an ethene/1-olefin copolymer depends strongly upon the molecular microstructure. With the development of modern single-site metallocene-based Ziegler-Natta catalysts a broad spectrum of olefin homopolymers and copolymers have become accessible. Metallocene-based Ziegler-Natta catalysts give excellent control of the copolymer molecular and supramolecular architecture with narrow molecular weight distribution and uniform comonomer incorporation for the entire feasible composition range.

In this study we prepared blends of isotactic and syndiotactic polypropenes (i-PP/s-PP) with poly(ethene-co-1-butene) (PEB) and investigated their morphologies and melt miscibility as a function of 1-butene content in PEB. For this purpose, we synthesized random PEB

copolymers with 1-butene contents varied from 11 to 100 wt.-%. The blends were investigated using atomic force microscopy, transmission electron microscopy, differential scanning calorimetry, X-ray scattering, and dynamic mechanical analysis. AFM phase imaging, a new fast developing method providing compositional mapping, has been used intensively to study the morphologies and nanostructures of the blends.

Results and Discussion

To investigate the i-PP/PEB melt miscibility behavior we prepared blends of i-PP with PEB52, PEB70, PEB82, PEB88 and i-P1B (the number associated with PEB indicates the wt.-% content of 1-butene, varied from 52, 70, 82, 88 to 100 wt.-%). The i-PP/PEB blends of composition 50/50 and 80/20 were prepared by mixing both components in a solution of xylene. The solvent free blends were annealed in the melt at 180 °C for 4h, and then cooled down to room temperature. The AFM phase images revealing the morphology of the blends were obtained on cryo-microtomed surfaces using a novel sample holder.¹¹⁾

As a representative example, Fig. 1a-c show the AFM phase images i-PP/PEB52, i-PP/PEB70 and i-PP/PEB88, respectively. AFM phase imaging (i.e., extension of tapping mode AFM, providing image contrast related to shifts in phase angles of vibration when the oscillating cantilever interacts with the sample surface) is a rather new, fast developing method which has been shown to provide enhanced image contrast and compositional maps related to local materials properties such as local surface stiffness and adhesion. In general, AFM phase image contrast depends in a complex way on sample properties and chosen experimental conditions.¹²⁾ The AFM phase images presented were taken under conditions which led to bright image contrast for the stiffer, more crystalline regions, i.e. i-PP, and to dark image contrast for the more compliant regions, i.e. PEB. Fig. 1a reveals a two-phase morphology with large, irregular domains up to several tens of micrometers in size. As the 1-butene content is increased from 52 to 70 and 88 wt.-% the size of the PEB rich domains decreases significantly. The AFM phase image of i-PP/PEB70 (Fig. 1b) shows that the size of the PEB rich domains does not exceed 2 μm in diameter, and as the 1-butene content is increased to 82 wt.-% the size of the PEB rich domains decreases below ≈ 200 nm (image not shown). For

the i-PP/PEB88 blend no phase separation can be observed as shown in Fig. 1c. Finally, for 100 wt.-% 1-butene content a two-phase morphology is observed (not shown).

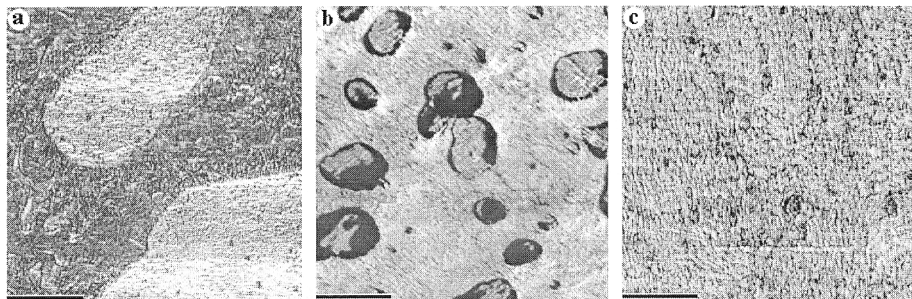


Fig. 1: AFM phase images of (50/50) i-PP/PEB blends. (a) 52 wt.-% 1-butene content, (b) 70 wt.-% 1-butene content, (c) 88 wt.-% 1-butene content. The horizontal bar corresponds to 2.8 μm in (a), 2.2 μm in (b) and 1.7 μm in (c).

The observed differences in domain sizes obviously indicate the different miscibility and compatibility of the i-PP/PEB blends. With increasing 1-butene content in PEB the amount of PEB included in the i-PP rich domains also increases resulting in smaller domains which finally disappear for ≈ 88 wt.-% 1-butene content. Based on the AFM results we investigated the i-PP/PEB88 blend in more detail by DSC, DMA and SAXS. The DSC measurements showed a considerable decrease of the melting temperature with increasing 1-butene content. The DMA data obtained for the i-PP/PEB88 blend showed a single $\tan \delta$ peak at -23 $^{\circ}\text{C}$ (between the $\tan \delta$ peaks of the homopolymers). These observations provide additional experimental evidence for miscibility, and thus we concluded a miscibility window for ≈ 88 wt.-% 1-butene content.¹³⁾

It is well known that s-PP shows a very different miscibility behavior than i-PP. Thus, it is of interest to study the miscibility of s-PP with PEB as a function of 1-butene content in PEB. We prepared blends of s-PP with PEB11, PEB20, PEB32, PEB52, PEB70, PEB82, PEB88 and i-P1B. The 70/30 s-PP/PEB blends were prepared by mixing both components in a solution of xylene. The solvent free blends were annealed in the melt at 180 $^{\circ}\text{C}$ for 4h, cooled down to room temperature and then isothermally crystallized for 24 h. Fig. 2a-c show representative AFM phase images for the s-PP/PEB20, s-PP/PEB82 and s-PP/i-P1B blends. The AFM images for all the s-PP/PEB blend samples under investigation revealed a two

phase morphology: the s-PP rich domains appear in bright contrast and the PEB rich regions form spherical or irregularly formed domains of dark contrast. Irregular PEB rich domains were found for the s-PP/PEB11, s-PP/PEB20 and s-PP/PEB32 samples (see Fig. 2a), and spherical domains were observed for the s-PP/PEB52, s-PP/PEB70, s-PP/PEB82, s-PP/PEB88 and s-PP/i-P1B samples (see Fig. 2b-c). The observation of irregular domains might be explained by the higher molecular weight and viscosity of PEB11, PEB20, and PEB32 (data not shown).

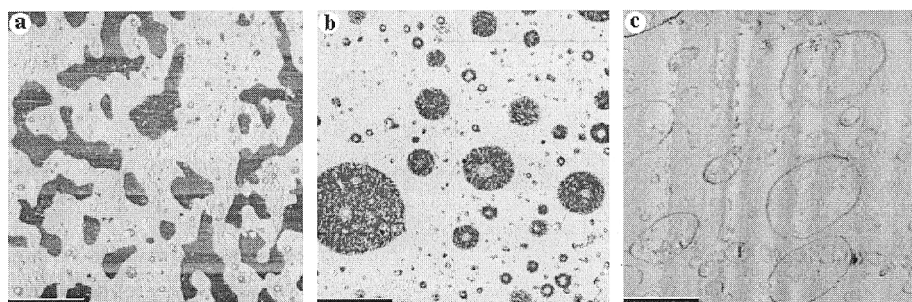


Fig. 2: AFM phase images of (70/30) s-PP/PEB blends. (a) 20 wt.-% 1-butene content, (b) 82 wt.-% 1-butene content, (b) 100 wt.-% 1-butene content. The horizontal bar corresponds to 3 μm in (a), (b) and (c).

Fig. 3a-c show AFM phase images for the s-PP/PEB20, s-PP/PEB82 and s-PP/PEB88 blends at higher magnification. For the s-PP/PEB52, s-PP/PEB70, s-PP/PEB82 and s-PP/PEB88 blends incorporation of s-PP in PEB rich domains was observed: s-PP fibrils and lamellae growing perpendicular at the s-PP/PEB domain interface (Fig. 3b-c show representative examples). s-PP/PEB11, s-PP/PEB20 and s-PP/PEB32 blend samples do not show any s-PP incorporation (Fig. 3a) and can be considered as immiscible. The different amount of s-PP incorporation in the PEB rich regions results in different structure and shape of the s-PP crystallites. For s-PP/PEB88 thin and long s-PP fibrils are formed and branching is quite absent (Fig. 3c). With increased s-PP incorporation the observed fibrils become thicker and more branched, and highly branched s-PP crystallites are observed for the s-PP/PEB52, s-PP/PEB70 and s-PP/PEB82 blend samples (Fig. 3b). A further increase of 1-butene content results in a decrease of the compatibility: although the phase image contrast between the crystalline s-PP and i-P1B regions is almost absent one can clearly observe an amorphous interface region of ≈ 50 nm thickness (Fig. 2c). Quantitative evaluation of the amount of incorporated s-PP in the PEB rich regions led to the conclusion of best compatibility for the s-

PP/PEB70 sample. Unlike for the i-PP/PEB case, miscibility was not observed for the s-PP/PEB blends studied in this work. This is also supported by DMA data which revealed two $\tan \delta$ peaks. We observed also a strong dependence of the morphologies on the thermal treatment. Blend samples which have been quenched to liquid nitrogen temperature showed worst compatibility while blend samples crystallized at 130 °C showed best compatibility. In conclusion, AFM phase imaging is a very powerful, new technique to study the morphology and miscibility of polyolefin blends.

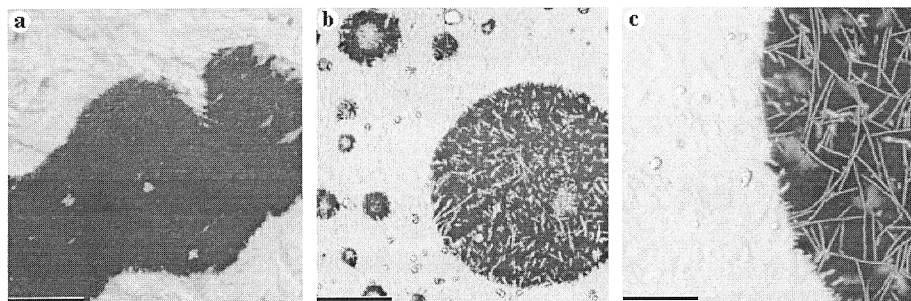


Fig. 3: AFM phase images of (70/30) s-PP/PEB blends. (a) 20 wt.-% 1-butene content, (b) 82 wt.-% 1-butene content, (c) 88 wt.-% 1-butene content. The horizontal bar corresponds to 0.4 μm in (a), 1.2 μm in (b) and 0.5 μm in (c).

References

1. W. W. Graessley, R. Krishnamoorti, G. C. Reichart, N. P. Balsara, L. J. Fetters, D. J. Lohse, *Macromolecules* **28**, 1260 (1995)
2. R. Krishnamoorti, W. W. Graessley, G. T. Dee, D. J. Walsh, L. J. Fetters, D. J. Lohse, *Macromolecules* **29**, 367 (1996)
3. F. S. Bates, G. H. Fredrickson, *Macromolecules* **27**, 3896 (1994)
4. P. A. Weimann, D. J. Todd, M. A. Hillmyer, F. S. Bates, *Macromolecules* **30**, 3650 (1997)
5. K. S. Schweizer, *Macromolecules* **26**, 6050 (1993)
6. J. Dudowicz, K. F. Freed, *Macromolecules* **24**, 5076 (1991)
7. K. F. Freed, J. Dudowicz, *Macromolecules* **31**, 6681 (1998)
8. M. Yamaguchi, H. Miyata, K.-H. Nitta, *J. Appl. Polym. Sci.* **62**, 87 (1996)
9. *Polypropylene Handbook*, E. P. Moore Jr., (Ed.), Hanser Publishers, Munich 1997
10. S. van der Ven, *Polypropylene and other Polyolefins*, Elsevier, Amsterdam, 1990
11. Y. Thomann, R. Thomann, M. Ganter, R. Machuta, G. Bar, R. Mülhaupt, *J. Microscopy* **195**, 161 (1999)
12. G. Bar, Y. Thomann, M.-H. Whangbo, *Langmuir* **14**, 1219 (1998)
13. Y. Thomann, J. Suhm, R. Thomann, R.-D. Maier, G. Bar, R. Mülhaupt, *Macromolecules* **31**, 5441 (1998)